Compositional Evolution During the Synthesis of FePt Nanoparticles

G. B. Thompson – The University of Alabama
Chandan Srivastava – The University of Alabama
David E. Nikles – The University of Alabama

Citation of published version:

Thompson, G., Srivastava, C., Nikles, D. (2008): Compositional Evolution During the Synthesis of FePt Nanoparticles. *Journal of Applied Physics*, 104(6).
DOI: https://doi.org/10.1063/1.2980042

Compositional evolution during the synthesis of FePt nanoparticles

Chandan Srivastava,[1] David E. Nikles,[2] and Gregory B. Thompson[1,a)]
[1]*Department of Metallurgical and Materials Engineering, The University of Alabama, Tuscaloosa, Alabama 35487, USA*
[2]*Department of Chemistry, The University of Alabama, Tuscaloosa, Alabama 35487, USA*

(Received 24 March 2008; accepted 21 July 2008; published online 25 September 2008)

A series of FePt nanoparticles was synthesized by the thermal decomposition of iron pentacarbonyl and reduction in platinum acetylacetonate in phenyl ether solvent. A range of precursor molar ratios of 2, 1.5, and 1 between iron pentacarbonyl and platinum acetylacetonate was studied. After 30 min of reflux, the synthesis method produced a wide distribution in composition and size for the nanoparticles. Given 200 min of reflux, it was observed that the particle-to-particle composition and size narrowed, and the atomic ratio of Fe to Pt, for the majority of nanoparticles, approached the initial precursor molar ratios except for the molar ratio of 1. It is speculated that the compositional variability may be a result of the slow kinetics of iron pentacarbonyl's decomposition in the reaction. © *2008 American Institute of Physics*. [DOI: 10.1063/1.2980042]

I. INTRODUCTION

In recent years there has been a tremendous effort toward decreasing the magnetic bit sizes to achieve higher magnetic areal information storage density. One proposed method for achieving ultrahigh storage density (>1 Tbit/in^2) is self-assembled arrays of FePt nanoparticles.[1] The $L1_0$ phase of FePt has high magnetocrystalline anisotropy that provides resistance to magnetic reversal caused by thermal energy fluctuations in small volumes.[2] Various chemical synthesis methods have been developed to produce FePt nanoparticles with good chemical stability.[2–4] The majority of these synthetic routes yields FePt nanoparticles with a metastable A1 structure.[2–4] To transform these nanoparticles to a magnetically hard $L1_0$ structure, the nanoparticles are annealed at temperatures of $\geq$550 °C.[5] The extent of subsequent structural transformation that occurs in these nanoparticles depends on their size[6] and composition.[7] Recent studies of FePt nanoparticles have shown a wide composition distribution between individual nanoparticles in an as-synthesized dispersion.[7,8] The distribution in composition indicates that only a fraction of nanoparticles in the dispersion have the equiatomic stoichiometry. This distribution in ratio of constituents can produce a variation in the structural and magnetic properties from particle to particle, severely affecting the quality of self-assembled arrays.

Yu *et al.*[7] and Srivastava *et al.*[8] showed that FePt nanoparticles produced by the reduction of platinum acetylacetonate [$Pt(acac)_2$] and the thermal decomposition of iron pentacarbonyl [$Fe(CO)_5$] result in a particle dispersion with a very high compositional variability. Nominally, this synthesis process, originally reported by Sun *et al.*,[2] involves approximately twice the stoichiometric amount of $Fe(CO)_5$ to $Pt(acac)_2$ in order to achieve an overall nanoparticle dispersion with an average equiatomic ratio. The needed increase in $Fe(CO)_5$ is believed to be a result of loss of some of the $Fe(CO)_5$ because of its highly volatile nature.[9] To date, there have been relatively few systemic studies on the nucleation and growth of these particles.[10,11] This paper reports how compositional variation initially develops and scales with particle size and how different Fe:Pt precursor molar ratios affect the particle-to-particle compositional variability over extended reflux times.

II. EXPERIMENTAL PROCEDURES

The nanoparticles in the present study were synthesized by the method similar to that of Sun *et al.*[2] In this process, various precursor amounts of $Pt(acac)_2$, given below, and 0.52 g of 1,2 hexadecanediol were mixed with 25 ml of phenyl ether in a 300 ml three neck round bottom flask. The flask was equipped with a magnetic stirrer and a reflux condenser. Nitrogen atmosphere was maintained inside the flask during the synthesis. The reaction mixture was heated to 100 °C, and at this temperature various precursor amounts of $Fe(CO)_5$, also given below, 0.5 mmol of oleic acid, and 0.5 mmol of oleyl amine were injected into the flask through a syringe. The temperature was then raised to the boiling point of the phenyl ether (~260 °C) and the reaction mixture was refluxed for different periods of time. After refluxing, the reaction mixture was allowed to cool to room temperature under a nitrogen atmosphere. Ethanol was then added to the reaction mixture to precipitate the nanoparticles. The nanoparticles were then cleaned (removal of surfactants for the electron microscopy studies) using the process described in Ref. 11. The resulting "clean" nanoparticles were then dispersed in hexane for further analysis.

To study the distribution in composition as a function of precursor ratio, the following amounts were used: (a) precursor molar ratio of 2; 1 mmol of $Fe(CO)_5$ and 0.5 mmol of $Pt(acac)_2$, (b) precursor molar ratio of 1.5; 0.75 mmol of $Fe(CO)_5$ and 0.5 mmol of $Pt(acac)_2$, and (c) precursor molar ratio of 1; 0.5 mmol of $Fe(CO)_5$ and 0.5 mmol of $Pt(acac)_2$. The phase of the nanoparticles was determined by x-ray diffraction (XRD) using a Rigaku 1-D/ MAX-2BX diffractometer operating at 40 kV and 40 mA with a Cu $k\alpha$ radiation

a)Electronic mail: gthompson@coe.eng.ua.edu.

source. The average composition of the nanoparticle dispersion was determined by x-ray energy dispersive spectroscopy (XEDS) analysis using a FEI XL-30 scanning electron microscope (SEM) operating at 20 kV. The SEM-XEDS has a larger interaction volume consequently yielding a larger sampling size for determining the average composition of the nanoparticle dispersion. The specimens for both the XRD and the SEM-XEDS analysis were prepared by drop drying the nanoparticle dispersion onto a Si wafer.

Bright field image acquisition and single nanoparticle composition measurements were done using a 200 keV field emission FEI Tecnai F20 Supertwin scanning transmission electron microscope (STEM). A highly dilute dispersion of the clean nanoparticles was drop dried onto a 50 nm thick silicon nitride supporting window for the TEM analysis. It should be noted that the nanoparticles suspended in the hexane dispersion were intentionally diluted to a large extent. The evaporation of hexane left large patches of self-assembled, similar sized particles and isolated, dispersed particles of different sizes on the TEM grid. These isolated particles, separated from each other by a distance greater than 25 nm, which did not assemble in any periodic arrangement because of their different sizes, were chosen for the size-composition correlation data reported.

The bright field TEM micrographs, captured on a 1k charge coupled device camera, were used to determine the size distribution of the nanoparticles in the dispersion. STEM-XEDS was used to determine the elemental compositions from individual nanoparticle. The nanoparticles were imaged in a *Z*-contrast imaging mode using a high angle annular dark field (HAADF) detector in STEM.[12] The STEM-XEDS analysis of the particles was performed with a FEI nano-beam spot size designation of 6, which corresponds to an XEDS spatial resolution of ~1.5 nm. The normal acquisition time for the analysis was 200 s with a drift correction at every 10 s during the acquisition. The presence of similar sized, self-assembled particles was used as the drift correction reference point for obtaining compositional information from the reported isolated particles.

For the elemental quantification, a background subtracted integrated intensity of peaks corresponding to Fe_K and Pt_L lines in the XEDS spectrum was used. The Cliff–Lorimer *k*-factor used for the elemental quantification of the nanoparticles was determined using a homogeneous FePt thin film whose composition was verified by Rutherford backscattering.[13] Bright field images of nanoparticles were used to determine the size and were correlated to the STEM-HAADF image for the elemental quantification.

III. RESULTS

The XRD curve for as-synthesized particles for all molar ratios and reflux times showed two broad peaks, the {111} peak near $2\Theta=40°$ and the {200} peak near $2\Theta=46°$, as shown in a representative curve in Fig. 1. This indicated that the particles were in the A1 phase.

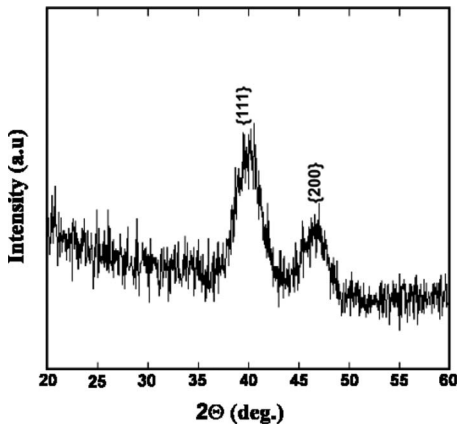

FIG. 1. A representative XRD curve for as-synthesized FePt nanoparticles. This particular XRD curve is for particles synthesized using the precursors in molar ratio of 2 and refluxed for 30 min.

A. Precursor molar ratio of 2

The size distribution histograms determined by TEM bright field micrographs for nanoparticles extracted after 30 and 200 min reflux are shown in Figs. 2(a) and 2(b), respectively. The average sizes for 30 and 200 min refluxed nanoparticles were 3.5 ± 0.9 nm and 3.7 ± 0.3 nm, respectively. The composition distribution histograms for nanoparticles in the dispersion extracted after 30 and 200 min reflux are shown in Figs. 2(c) and 2(d), respectively. The composition for the 30 min refluxed nanoparticles ranged from 21 to 94 at. % Pt with a mean value of 56 ± 15 at. % Pt. This composition value was in good agreement with the SEM-

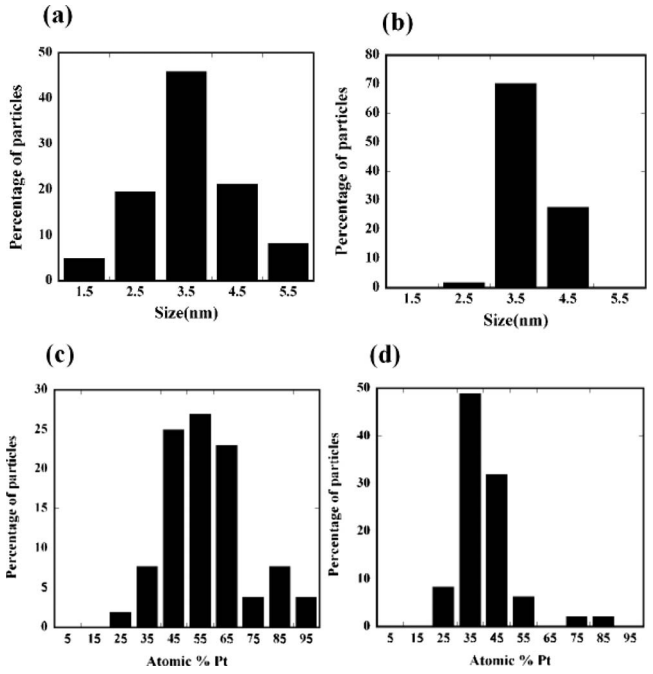

FIG. 2. Histogram plots for particles extracted from the reaction mixture containing the precursors in molar ratio of 2 and corresponding to (a) size distribution after 30 min reflux, (b) size distribution after 200 min reflux, (c) composition distribution after 30 min reflux, and (d) composition distribution after 200 min reflux. Total number of individual nanoparticles analyzed for the compositional analysis was 52 for 30 min reflux and 47 for 200 min relfux.

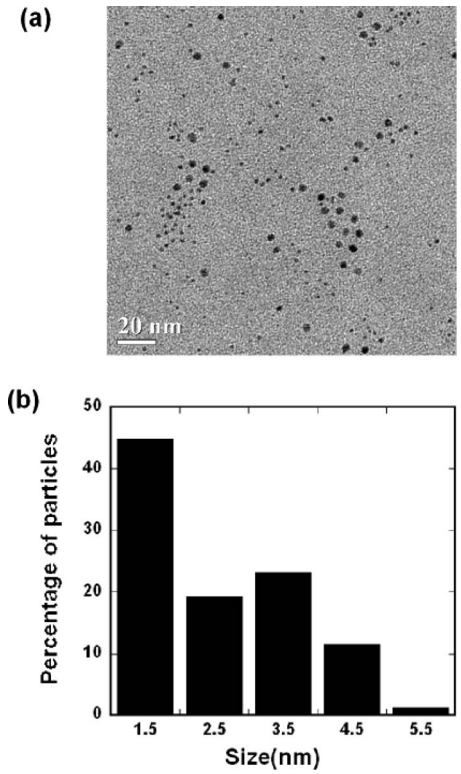

FIG. 3. (a) Bright field image and (b) size distribution histogram of particles extracted at 160 °C from the reaction mixture containing precursors in molar ratio of 2. Total number of particles analyzed was 100.

XEDS analysis value of 55 at. % Pt. For the particle dispersion extracted after 200 min reflux, the composition range was from 25 to 86 at. % Pt with a mean value of 42 ± 10 at. % Pt. Similar as above, this value was in good agreement with the average composition of 47 at. % Pt determined from the SEM-XEDS analysis.

In particular to this molar ratio, a detailed study of the size-composition relationship was performed for nanoparticles extracted from the reaction mixture at 160 °C (i.e., seed particle formation stage) and after 30 min of reflux at 260 °C. This ratio was chosen because of its greater variability in composition during the early stages of synthesis, as compared to the other molar ratios given below. Also, this molar precursor ratio has been commonly chosen in the synthesis of these nanoparticles in the literature.[5,11,14,15]

The TEM bright field and size distribution histogram for the nanoparticles extracted from the reaction vessel at 160 °C are shown in Figs. 3(a) and 3(b). The average size determined from the bright field TEM micrographs was 2.6 ± 1.03 nm with a range from ≈1 to ≈5 nm. Imaging the nanoparticle dispersion in STEM-HAADF mode revealed bright and dull contrast particles, as shown in Fig. 4(a). The compositions of groups of bright and dull contrast particles were determined from different regions on the TEM grid. The measurements from ten different regions containing groups of ≈15 particles revealed that the bright particles were Pt rich with an average composition of $Fe_{24}Pt_{76}$, and the dull particles were Fe rich with an average composition of $Fe_{82}Pt_{18}$. This composition dependent variation, in contrast, for nearly similar sized nanoparticles, is consistent with the

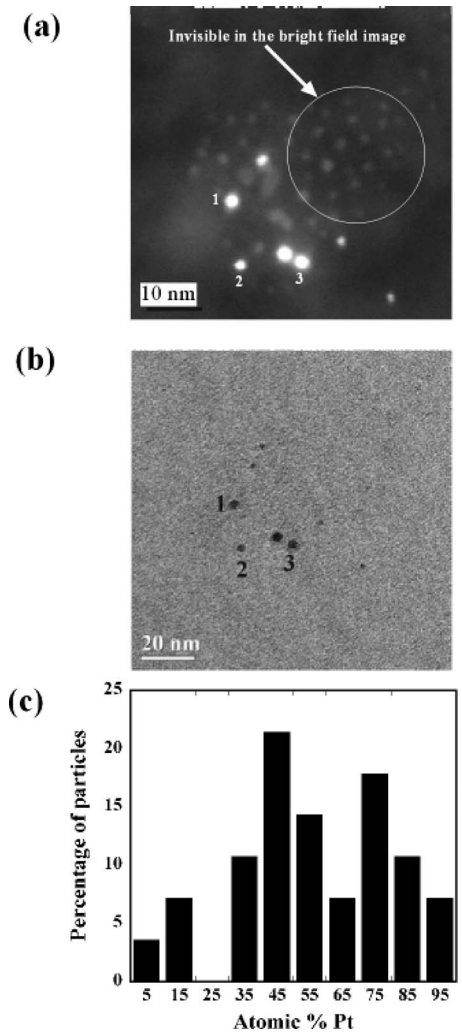

FIG. 4. (a) A representative STEM image showing the presence of the bright and dull contrast particles in dispersion extracted at 160 °C from the reaction mixture containing the precursors in molar ration of 2. (b) Bright field image of the same region on the sample grid illustrating the invisibility of the dull contrast particles in the TEM bright field mode. Note the numbered nanoparticles between (a) and (b). (c) Composition distribution histogram obtained from the analysis of 32 individual particles for nanoparticle dispersion extracted at 160 °C.

Z-contrast imaging mode of the HAADF detector.[12] Interestingly, it was noticed that the dull contrast particles visible in the STEM-HAADF mode were undetectable in the bright field mode. The STEM-HAADF micrograph shown in Fig. 4(a) when compared to the bright field micrograph of the same region shown in Fig. 4(b) clearly illustrates this observation. It should be noted that only the bright field micrographs, and not the STEM-HAADF, were used for determining the average size and size distribution of the particles in the 160 °C extracted dispersion. This was done to avoid any error in the size estimate of the particles that could be produced by nonoptimal contrast or brightness adjustments in the STEM-HAADF mode. We noted that the hue around the particles varied slightly with contrast/brightness changes, which could result in inaccurate size measurement in this imaging condition. This led to the counting of mostly Pt rich (visible in bright field mode) particles in the 160 °C ex-

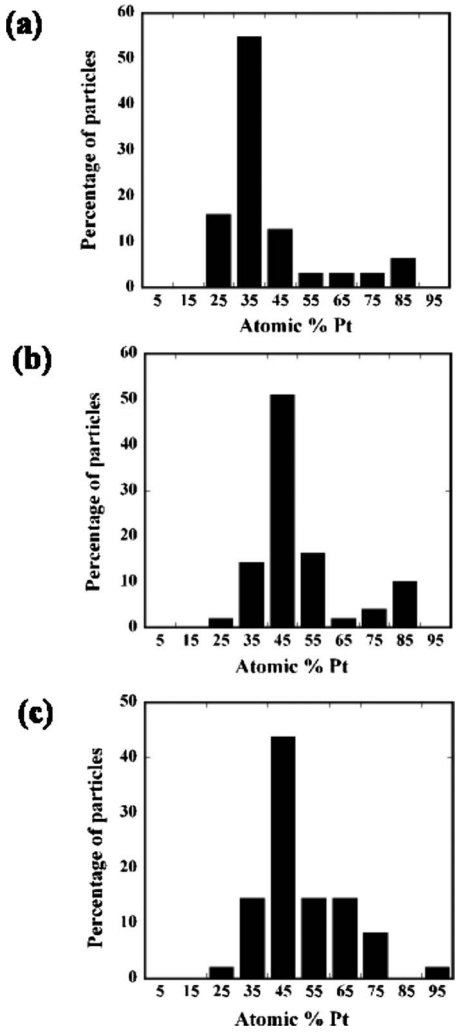

FIG. 5. Distribution of composition for FePt nanoparticles, synthesized using precursors in molar ratio of 2, for sizes (a) 1.5 to ≤3 nm, (b) 3 to ≤4 nm, and (c) 4 to ≤5.5 nm. Total number of particles analyzed in each size range can be found in Table I.

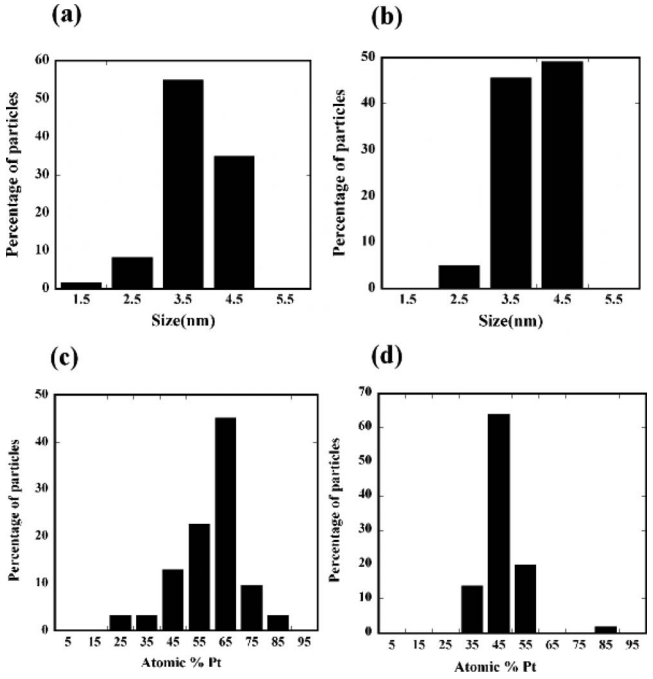

FIG. 6. Histogram plots for particles from the reaction mixture containing the precursors in molar ratio of 1.5 and corresponding to (a) size distribution after 30 min reflux, (b) size distribution after 200 min reflux, (c) composition distribution after 30 min reflux, and (d) composition distribution after 200 min reflux. Total number of particles analyzed for the compositional analysis was 32 for 30 min reflux and 50 for 200 min reflux.

tracted dispersion for the size related analysis. The single nanoparticle composition distribution for the specimen extracted at 160 °C is plotted in Fig. 4(c).

The nanoparticle dispersion of the size-composition correlation analysis for the precursor molar ratio of 2 after 30 min of reflux was divided into three size ranges: (a) range 1: 1.5 to ≤3 nm, (b) range 2: 3 to ≤4 nm, and (c) range 3: 4 to ≤5.5 nm. The composition distribution histograms shown in Figs. 5(a)–5(c)correspond to each of these three ranges, respectively. The total number of particles analyzed and the average compositions for these particles (determined from the summation average of the individual nanoparticle's compositions) in each range is tabulated in Table I. The binning of data into the three size ranges was based on the abundance of the analyzed particles in the respective size range and was not done for any intentional statistical purpose.

B. Precursor molar ratio of 1.5

The nanoparticle size distribution histograms determined by TEM bright field micrographs for nanoparticles extracted after 30 and 200 min reflux are plotted in Figs. 6(a) and 6(b), respectively. The average sizes for 30 and 200 min refluxed particles were 3.6 ± 0.6 and 3.8 ± 0.5 nm, respectively. Composition distribution histograms for particles in the dispersion extracted after 30 and 200 min reflux are shown in Figs. 6(c) and 6(d), respectively. The composition for 30 min refluxed particles ranged from 27 to 81 at. % Pt with a mean value of 58 ± 12 at. % Pt. This composition value was in good agreement with the SEM-XEDS analysis value of 56 at. % Pt. For the particle dispersion extracted after 200 min reflux, the composition range was from 35 to 87 at. %

TABLE I. This table shows the analysis values for nanoparticle dispersion extracted after 30 min of reflux from the reaction mixture containing the precursors in a molar ratio of 2, the total number of nanoparticles analyzed, average composition (determined from the average of individual particle's compositions), and composition range for the particles in each size range.

Size range	Number of particles analyzed	Average size in nm (standard deviation)	Average composition in at. % Fe (standard deviation)	Composition range in at. % Fe
1.5–3 nm	32	2.3(0.410)	58 (15)	10–73
3–4 nm	50	3.5(0.248)	48 (14.6)	14–70
4–5.5 nm	48	4.5(0.376)	47 (13.7)	7–73

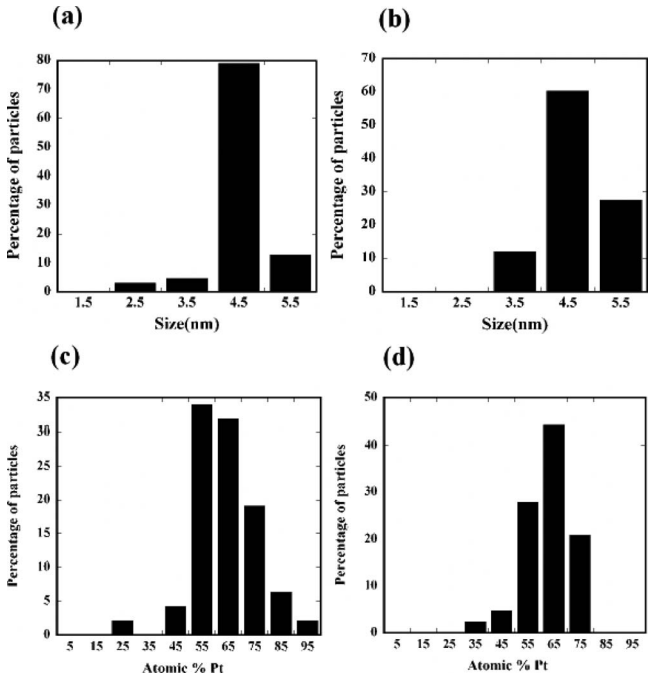

FIG. 7. Histogram plots for particles extracted from the reaction mixture containing the precursors in molar ratio of 1 and corresponding to (a) size distribution after 30 min reflux, (b) size distribution after 200 min reflux, (c) composition distribution after 30 min reflux, and (d) composition distribution after 200 min reflux. Total number of particles analyzed for the compositional analysis was 50 for 30 min reflux and 50 for 200 min reflux.

Pt with a mean value of 46 ± 7 at. % Pt. Again, this value was in good agreement with the average composition of 52 at. % Pt determined from the SEM-XEDS analysis.

C. Precursor molar ratio of 1

TEM bright field micrographs were used to determine the nanoparticle sizes after 30 and 200 min reflux. The size distribution histograms for these particles are plotted in Figs. 7(a) and 7(b), respectively. The average sizes for 30 and 200 min refluxed particles were 4.5 ± 0.5 and 4.6 ± 0.6 nm, respectively. Composition distribution histograms for the particles in dispersions extracted after 30 and 200 min reflux are shown in Figs. 7(c) and 7(d), respectively. The composition for 30 min refluxed particles ranged from 21 to 90 at. % Pt with a mean value of 63 ± 12 at. % Pt. This composition value was in good agreement with the SEM-XEDS analysis value of 64 at. % Pt. For the particle dispersion extracted after 200 min reflux, the composition range was from 37 to 79 at. % Pt with a mean value of 61 ± 9 at. % Pt. Again, this value was in good agreement with the average composition of 63 at. % Pt determined from the SEM-XEDS analysis.

IV. DISCUSSION

It has been widely practiced that for producing an average equiatomic FePt nanoparticle dispersion using the method of Sun *et al.*,[2] the molar ratio of $Fe(CO)_5$ and $Pt(acac)_2$ should be 2.[2,5,11,14,15] In this study, it was observed that using a precursor molar ratio of 2 and a reflux time of 30 min produced particles with an average composition of about

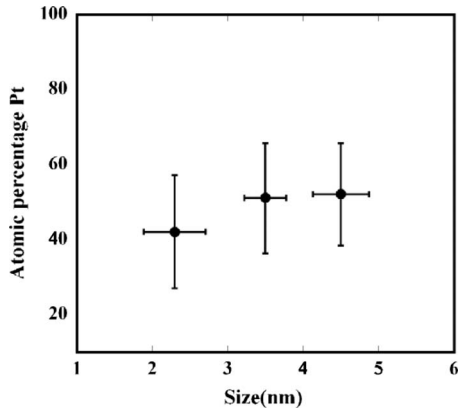

FIG. 8. Variations in atomic percentage of Pt with the size of the particles for the 30 min reflux FePt nanoparticle dispersion synthesized using the precursor molar ratio of 2. The *x*-axis bar represents one standard deviation of particle size and the *y*-axis bar represents one standard deviation of composition from the mean value.

55 at. % Pt, in agreement with the already reported results.[5,11] However, the analysis at the individual nanoparticle level revealed a wide distribution in compositions between particles for the same dispersion, as shown in Fig. 2(c). It is evident from the composition histogram in Fig. 2(c) that the nanoparticle dispersion contains a large number of Pt rich particles, some Fe rich particles, and particles having equiatomic stoichiometry. Bagaria *et al.*[11] reported that the dominant mechanism of formation of nanoparticles by the Sun *et al.*[2] synthesis process involves the heterogeneous nucleation of Fe onto these Pt rich clusters. The presence of a large number of Pt rich particles in the dispersion after 30 min reflux indicates that either the initial amount of Fe precursor $[Fe(CO)_5]$ is depleted or the reflux time is insufficient, which will be addressed in detail below.

In the analysis of the composition distribution for the precursor molar ratio of 2, the nanoparticle dispersion extracted at 30 min reflux showed that the smaller nanoparticles (range 1) were Fe rich, with the majority having a composition of ≈35 at. % Pt. The nanoparticles in ranges 2 and 3 had similar composition distribution with maximum percentage of nanoparticles having a composition closer to the average value of ≈51 at. % Pt. This result is plotted in Fig. 8. The standard deviation of distribution in each range had a similar value of about 15 at. % Pt, indicating a significant variability in composition within each size range. Although the mean value of composition for the smallest size nanoparticles was Fe rich, each range's average composition was within one standard deviation. This suggests that there does not exist a strong size-composition dependency for these nanoparticles. But the mean values may suggest some trends in which nanoparticles favor growth during the synthesis.

The presence of 1,2 hexadecanediol in the reaction mixture causes a faster reduction of $Pt(acac)_2$ and the formation of Pt rich clusters during the early stages as compared to the slower thermal decomposition of $Fe(CO)_5$. However, this paper has clearly shown that Fe rich seeds do form in these early stages. As the Fe atoms are continuously produced by the slower decomposition of $Fe(CO)_5$, these Fe atoms can

TABLE II. This table lists the average size with standard deviation, composition range, and average composition with standard deviation for nanoparticles synthesized using different ratios of precursors and refluxed for 30 and 200 min.

Molar ratio of precursors ($Fe(CO)_5$/Pt(acac)2)	Reflux time (minutes)	Average size (nm) ± standard deviation	Composition (at% Pt)	
			Range	Average ± standard deviation
2	30	3.5± 0.9	21–94	56±15
	200	3.7± 0.3	25–86	42±10
1.5	30	3.6± 0.6	27–81	58±12
	200	3.8± 0.5	35–87	46±7
1	30	4.5± 0.5	21–90	63±12
	200	4.6± 0.6	37–79	61±9

either nucleate on the surface of existing Fe rich particle or onto a Pt rich particle. Srivastava *et al.*[8] reported a Monte Carlo simulation based free energy perturbation (FEP) calculation study on the extent of Fe diffusion into the core of a 2 nm Pt seed particle. The FEP calculations have predicted the thermodynamic equilibrium concentration for the diffusion of Fe atoms into a 2 nm Pt cluster to be ~43 at. % Fe. In the 30 min reflux dispersion, the higher count of small size (≤2 nm) Fe rich particles and the lower number of similar sized Pt rich particles suggest that the Pt rich particles preferentially grow as compared to Fe rich particles. The diffusion of Fe into the subsurface of a Pt cluster would be energetically preferable as it minimizes the higher surface energy configuration of Fe atoms on the surface of another Fe rich particle. Therefore, the small Fe rich particles present in the 30 min reflux dispersion are believed to be the ones that nucleated during the early stages of the synthesis and did not grow in the subsequent stages. By avoiding the supersaturation of the Fe species that produces Fe rich clusters during the initial stage of synthesis, it is speculated that the compositional and size distribution will be narrower for the same reflux time. Changing the release sequence of iron from iron pentacarbonyl during the synthesis is the subject of future studies.

Interestingly, it was observed that increasing the reflux time to 200 min resulted in the narrowing of the composition distribution. The decrease in Pt rich particles, as shown in Figs. 2(c) and 2(d), indicates that the Fe requires sufficiently longer reflux time to be incorporated in the FePt nanoparticles. It is suspected that the Fe could form metal-organic complexes with the surfactants, thereby being able to remain in the reaction mixture after thermally decomposing from the $Fe(CO)_5$ source, or alternatively, the Fe may have formed small Fe rich seeds that experience restricted growth based on the Monte Carlo simulations referenced above.[8] The STEM-HAADF micrographs of the dispersion after 200 min of reflux did not indicate any dull contrast (Fe rich) particles. This further suggests that these Fe rich clusters have attached to the Pt rich particles providing the Fe source for the narrowing of the composition. Interestingly, the attachment of these clusters to the nanoparticles, if it is the mechanism, did not statistically increase in the mean particle size between the 30 and 200 min reflux times. The narrowing of the composition to ~35 at. % Pt with a decrease in the standard deviation, as shown in Fig. 2(d), indicates that given appropriate time, the system will approach the molar composition of the precursors, i.e., 2 Fe to 1 Pt.

The composition distribution analysis for nanoparticles synthesized using 1:1 and 1.5:1 molar ratios of $Fe(CO)_5$ and $Pt(acac)_2$ was then used to determine if the precursor molar ratio with appropriate reflux time can achieve a narrow composition distribution at a targeted average value. For the precursor molar ratio of 1.5, it was observed that the particles after 30 min reflux exhibited a characteristically wide composition distribution with an average value of 58 ± 12 at. % Pt. Increasing the reflux time to 200 min resulted in the narrowing of composition distribution to 46 ± 7 at. % Pt. Again, as seen in the molar ratio of 2, this narrowing of composition at 46 at. % Pt is in reasonable agreement with the stoichiometrically calculated composition of $Fe_{60}Pt_{40}$ for 1.5 mmol of $Fe(CO)_5$ and 0.5 mmol of $Pt(acac)_2$.

For the nanoparticles synthesized using 1:1 precursor molar ratio, it was observed that most of the nanoparticles in the reaction mixture after 30 min reflux were Pt rich with an average value of 63 ± 12 at. % Pt, as seen in Fig. 7(c). This result is again consistent with the previous trends. Surprisingly, it was observed that an increase to 200 min of reflux yielded particle dispersion with an average composition of 61 ± 9 at. % Pt and did not produce any significant change in the composition distribution or the average composition of the dispersion after 30 min. This dispersion was then further refluxed for 500 min, which also did not produce any significant change in the previous average composition value. This result indicates a potential limit in achieving a targeted composition with the precursor ratio and reflux time methods. The lack of narrowing of the composition to the desired equiatomic ratio is believed to be a result of the loss of $Fe(CO)_5$ during the reaction because of its highly volatile nature.[9] The reaction mixture containing the precursors in molar ratio of 1.5, although narrowed, was also not able to achieve the targeted composition value of 40 at. % Pt, further suggesting a trend in the loss of Fe from the reaction mixture.

V. CONCLUSION

In the present study, FePt nanoparticles were produced by using different molar ratios of the precursors and reflux times. A tabulation of the collective results is given in Table

II. If the reaction mixture is refluxed for an extended time period and if there is a sufficient availability of precursors not lost during the reaction, the composition narrows to a value approximately equal to the molar ratio of the precursors. This result is particularly relevant for the common practice of a 2:1 ratio of $Fe(CO)_5$ and $Pt(acac)_2$. The slow and volatile nature of the $Fe(CO)_5$ decomposition results in a wide size and composition dispersion in the early stages of nucleation and growth. For groups of similar sized particles, the mean composition value after 30 min of reflux was all within one standard deviation of each other. This indicates that a strong size-composition correlation does not exist for the nanoparticles synthesized by this process. Extended periods of refluxing up to 200 min did result in the eventual narrowing of the composition distribution in the 2:1 molar ratio. It is speculated that the initial Fe rich clusters that form in the early stages of synthesis are given sufficient time to eventually attach to the larger Pt rich nanoparticles during the extended reflux period. This is concluded by the Fe rich particles' conspicuous absence in the 200 min reflux dispersion when imaged in the HAADF-STEM mode. As the precursor ratio approaches 1, the particles are not able to achieve the targeted molar ratios of the precursors even at extended reflux times because of the loss of Fe from the volatile nature of the $Fe(CO)_5$.

ACKNOWLEDGMENTS

The authors gratefully acknowledge the National Science Foundation Materials Research Science & Engineering Center (Grant No. DMR-0213985) for supporting this work. The Tecnai TEM was acquired through the National Science Foundation Major Instrumentation Program (Grant No. DMR-0421376). Dr. Claudiu I. Muntele and Dr. Daryush Ila from the Center for Irradiation of Materials, Alabama A&M University are thanked for the RBS analysis. The authors also acknowledge the University of Alabama Materials Science Graduate Fellowship Program for additional support.

[1] R. F. C. Farrow, D. Weller, R. F. Marks, M. F. Toney, A. Cebollada, and G. R. Harp, J. Appl. Phys. **79**, 5967 (1996).
[2] S. Sun, C. B. Murray, D. Weller, L. Folks, and A. Moser, Science **287**, 1989 (2000).
[3] S. Sun, S. Anders, T. Thomson, J. E. E. Baglin, M. F. Toney, H. F. Hamann, C. B. Murray, and B. D. Terris, J. Phys. Chem. B **107**, 5419 (2003).
[4] S. Sun and H. Zeng, J. Am. Chem. Soc. **124**, 8204 (2002).
[5] Z. R. Dai, S. Sun, and Z. L. Wang, Nano Lett. **1**, 443 (2001).
[6] M. Tanase, N. T. Nuhfer, D. E. Laughlin, T. J. Klemmer, C. Liu, N. Shukla, X. Wu, and D. Weller, J. Magn. Magn. Mater. **266**, 215 (2003).
[7] A. C. C. Yu, M. Mizuno, Y. Sasaki, and H. Kondo, Appl. Phys. Lett. **85**, 6242 (2004).
[8] C. Srivastava, J. Balasubramanian, C. H. Turner, J. M. Wiest, H. G. Bagaria, and G. B. Thompson, J. Appl. Phys. **102**, 104310 (2007).
[9] T. J. Klemmer, N. Shukla, C. Liu, X. W. Wu, E. B. Svedberg, O. Mryasov, R. W. Chantrell, and D. Weller, Appl. Phys. Lett. **81**, 2220 (2002).
[10] M. Chen, J. P. Liu, and S. Sun, J. Am. Chem. Soc. **126**, 8394 (2004).
[11] H. G. Bagaria, D. T. Johnson, C. Srivastava, G. B. Thompson, M. Shamsuzzoha, and D. E. Nikles, J. Appl. Phys. **101**, 104313 (2007).
[12] E. Carlino and V. Grillo, Phys. Rev. B **71**, 235303 (2005).
[13] J. C. Barbour, K. Sikafus, and M. Nastasi, J. Vac. Sci. Technol. A **3**, 1895 (1985).
[14] H. Zeng, S. Sun, R. L. Sandstrom, and C. B. Murray, J. Magn. Magn. Mater. **266**, 227 (2003).
[15] S. Sun, E. E. Fullerton, D. Weller, and C. B. Murray, IEEE Trans. Magn. **37**, 1239 (2001).